Synthesis, structure, and excited state kinetics of heteroleptic Cu(I) complexes with a new sterically demanding phenanthroline ligand

*Lars Kohler, Dugan Hayes, Lin X. Chen, and Karen L. Mulfort**

Division of Chemical Sciences and Engineering, Argonne National Laboratory, 9700 South Cass Avenue, Argonne, IL 60439

*To whom correspondence should be addressed. E-mail: mulfort@anl.gov

RECEIVED DATE

ABSTRACT

In this report we describe the synthesis of a new phenanthroline ligand, 2,9-di(2,4,6-tri-isopropyl-phenyl)-1,10-phenanthroline (**bL2**) and its use as the blocking ligand in the preparation of two new heteroleptic Cu(I)diimine complexes. Analysis of the CuHETPHEN single crystal structures shows a distinct distortion from ideal tetrahedral geometry around the Cu(I) center, forced by the secondary phenanthroline ligand rotating to accommodate the isopropyl groups of **bL2**. The increased steric bulk of **bL2** as compared to the more commonly used 2,9-dimesityl-1,10-phenanthroline blocking ligand prohibits intramolecular ligand-ligand interaction, which is unique among CuHETPHEN complexes. The ground state optical and redox properties of CuHETPHEN complexes are responsive to the substitution on the blocking ligand even though the differences in structure are far removed from the Cu(I) center. Transient optical spectroscopy was used to understand the excited state kinetics in both coordinating and non-coordinating solvents following visible excitation. We have found that substitution of the blocking phenanthroline ligand has a significant impact on the ^{3}MLCT decay and can be used to increase the excited state lifetime by 50%. This work contributes to the growing library of CuHETPHEN complexes and broadens the fundamental understanding of their ground and excited state properties.

Introduction

Toward the development of multi-functional molecular architectures, the structural diversity possible within transition metal coordination complexes presents an enormous potential to direct and tune the physical and chemical properties governing behavior.[1-4] Certainly the metal centered states guide the redox and optical properties of a complex, but the inner and outer sphere ligand environment surrounding the metal center also play a significant role in the molecule's response to external stimuli and chemical reactivity.[5-14] Transition metal coordinating ligands can be used to directly link complementary functionalities (i.e. light absorption and catalysis) in mono- or multi-metallic complexes and direct intra- vs. inter-molecular interactions.[15] Additionally, coordinating ligands will influence the dimensionality of *supra*molecular architectures and can be used to build up multidimensional molecular materials, coordination polymers, and extended crystalline frameworks from discrete molecules.[16-26] For these reasons, we are interested in developing new metal-coordinating ligands to explore their impact on molecular and supramolecular structure, ground and excited state properties, and photochemical reactivity.

Copper(I)diimine complexes hold significant promise as earth-abundant light-absorbing modules in systems for solar energy conversion.[27-28] Importantly, Cu(I)bis(1,10-phenanthroline) complexes exhibit similar optical absorbance in the visible region to the more commonly used and well-understood Ru(II)tris(2,2'-bipyridyl) photosensitizers, even though the excited state lifetimes of Cu(I)$(phen)_2$ complexes are typically orders of magnitude shorter than their Ru(II) counterparts.[29-30] Homoleptic Cu(I)$(phen)_2$ complexes have been studied by a variety of optical and X-ray spectroscopies to fully understand this pronounced difference in excited state kinetics and the influence of unusual light-induced structural dynamics.[31-32] This work has formed the basis for a common excited state decay pathway which occurs through three distinct steps following excitation of the metal-to-ligand charge transfer (MLCT) transition. First, light-induced formation of the ^{1}MLCT excited state is followed by a flattening distortion from tetrahedral geometry in the $3d^{10}$ Cu(I) ground state to roughly square planar in the $3d^9$ Cu(II) ^{1}MLCT state. The time constant for this process, τ_1, is generally sub-picosecond. Next, the flattened ^{1}MLCT state undergoes intersystem crossing (ISC) to yield the triplet excited state (^{3}MLCT), which usually

occurs with a time constant (τ_2) between 4 and 20 picoseconds. Last, the flattened ^{3}MLCT state relaxes back to ground state, and the kinetics of this process are highly dependent on the solvent (coordinating vs. non-coordinating) and accessibility of the Cu(II) center to solvent approach. Decay of the ^{3}MLCT state (τ_3) ranges from 20 ps for Cu(I)(1,10-phenanthroline)$_2$ to well over 2 μs for the highly substituted Cu(I)(2,9-di(sec-butyl)-3,4,7,8-tetramethyl-1,10-phenanthroline)$_2$[33-34] which exploits cooperative interaction between the substituents of the phenanthroline ligands.[35] Overall, the structural factors that influence the excited state kinetics and dynamics are quite well understood for homoleptic Cu(I)(phen)$_2$ complexes. However, by comparison, there is a distinct lack of information regarding the excited state properties of well-defined *hetero*leptic Cu(I)bis(phenanthroline), or CuHETPHEN, complexes.

Looking to expand the fundamental understanding of the physical properties of CuHETPHEN complexes, our group recently reported the detailed characterization of the ground state and the ultrafast excited state dynamics of several CuHETPHEN model complexes.[36] Employing the most common strategy for CuHETPHEN synthesis, we used 2,9-dimesityl-1,10-phenanthroline as a sterically bulky blocking ligand (**bL**) to allow coordination of a second phenanthroline ligand (**L**) on which we varied the substitution adjacent to Cu(I), extended the phenanthroline conjugation, and added epoxide groups as facile handles for subsequent functionalization. We found that the excited state lifetime in acetonitrile can be tuned over two orders of magnitude within this family and is largely dictated by the steric bulk of the 2,9-substitution of **L**. Meanwhile, Odobel and co-workers have made impressive use of the HETPHEN synthesis methodology in the development of linked electron donor—CuHETPHEN—acceptor triads and adsorbed CuHETPHEN sensitizers to TiO_2 nanoparticles to measure charge injection in models of dye-sensitized solar cells.[37-38]

In this report, we have synthesized a new phenanthroline ligand and used it to access two new CuHETPHEN model complexes (Figure 1). The new ligand increases the steric bulk at the 2,9-phenanthroline position of **bL** from the typically used 2,4,6-trimethyl-phenyl (**bL1**) to 2,4,6-triisopropyl-phenyl (**bL2**). We postulated that the larger isopropyl groups of **bL2** would increase the excited state lifetime of the CuHETPHEN complexes by 1) more effectively blocking solvent access to the Cu(II) center in the ^{3}MLCT state, and 2) preventing the intramolecular π-π

interactions between phenanthroline ligands that we observed by single crystal analysis of **bL1** based CuHETPHEN complexes. As we will demonstrate using the new CuHEPHEN complexes based on **bL2**, the environment immediately surrounding the Cu(I) center influences its optical and redox properties as well as its excited state kinetics. In addition to the CuHETPHEN complexes described here, we note that sterically crowded coordinating ligands have use in complexes of many transition metals to modify the chemical reactivity and that this new ligand could certainly find potential applications in a number of different areas.

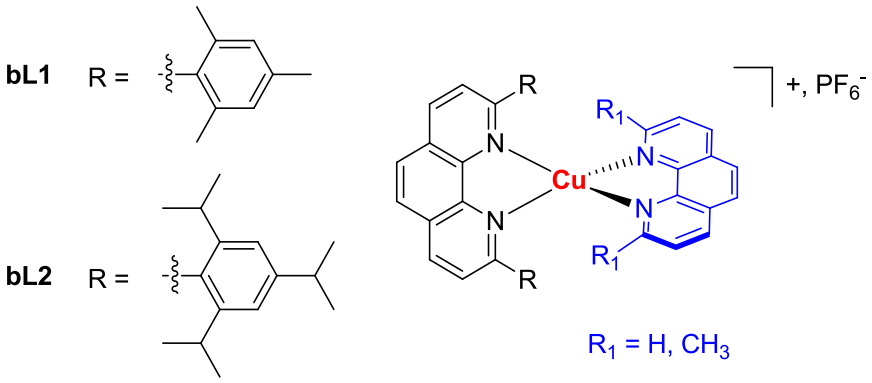

Figure 1. Relevant features of CuHETPHEN complexes studied in this work. Blocking ligand (**bL**) shown in black and the second 1,10-phenanthroline ligand shown in blue.

Experimental

General materials and methods. All reagents and solvents were purchased from commercial sources and were used as received. Complexes **1** and **2** and 2,9-dichloro-1,10-phenanthroline were prepared following previously published procedures.

^{1}H NMR was performed on a Bruker DMX 500 and referenced to TMS or residual solvent peak. ESI-MS was collected on a ThermoFisher LCQ Fleet from dilute methanol solutions in positive ionization mode. Elemental analysis was performed by Midwest Microlab, LLC (Indianapolis, IN, USA). UV-Vis absorption measurements were performed on a Beckman Coulter DU800 spectrophotometer. Steady state emission spectra were measured on a Quantamaster spectrophotometer from Photon Technology International; each sample was dissolved in spectrophotometric grade dichloromethane and thoroughly de-aerated with N_2.

Cyclic voltammetry. Cyclic voltammetry was conducted using a standard three-electrode cell on a BioAnalytical Systems (BAS) 100B potentiostat and cell stand with a 3 mm-diameter glassy carbon working electrode, a Pt wire auxiliary electrode, and a pseudo Ag/AgCl reference

electrode. Each solution in anhydrous dichloromethane was purged with N_2 prior to measurement and maintained under a blanket of N_2 during measurement. Tetrabutylammonium hexafluorophosphate (0.1 M) was used as the supporting electrolyte. Ferrocene (purified by sublimation) was added as an internal standard and redox potentials were referenced to the ferrocene/ferrocenium couple (0.46 V vs. SCE (dichloromethane)).[39] All scans were performed at 100 mV s^{-1}.

Single crystal X-ray diffraction. Crystals suitable for single crystal X-ray diffraction measurements were affixed to glass micropipettes using a quick drying two-part epoxy and their diffraction patterns collected on a Bruker SMART diffractometer equipped with an APEXII CCD detector using Mo K_a radiation. An Oxford Cryosystems 700 series cryostat was used for controlling the sample temperature. Data were corrected for absorption using SADABS. Structure solutions and structure refinements on F^2 were carried out using SHELXS and SHELXL, respectively. The crystal structures of **3** and **4** are deposited at the Cambridge Crystallographic Data Centre as structures 1515480 and 1515481.

Transient absorption spectroscopy. Femtosecond transient absorption measurements were performed using an amplified Ti:Sapphire laser system (Spectra Physics, Spitfire Pro) and an automated data acquisition system (Ultrafast Systems, Helios). The amplifier was seeded with the 100 fs output from the oscillator (Spectra Physics, Mai Tai) and was operated at 1.0 kHz, giving 3 mJ pulses centered at 830 nm. The beam was split 90/10, with the weaker beam being used to generate the white light continuum probe. The probe beam was delayed relative to the pump with a retroreflector mounted on a motorized delay stage and focused into a sapphire plate to generate a white light continuum spanning 420 to 650 nm. The continuum probe was focused to a spot size of 200 μm at the sample and subsequently focused into a fiber optic coupled to a multichannel spectrometer and CMOS sensor. The other 830 nm beam was focused into a BBO crystal to generate the 415 nm pump beam used for the pump-probe measurements. This beam was passed through a depolarizer, chopped at 500 Hz, focused at the sample position to a spot size of 400 μm, and attenuated to a pulse energy of 0.5 μJ. Transient absorption spectra were collected using the Helios control software. The data were corrected for temporal chirp in the probe beam using the separately collected nonresonant response of the blank solvent. The

nonresonant response gave an instrument response time of approximately 300 fs. All experiments were performed at room temperature with constant stirring with samples in 2 mm quartz cuvettes that had been bubbled with nitrogen.

Nanosecond transient absorption spectroscopy was measured at the Center for Nanoscale Materials at Argonne National Laboratory using an amplified Ti:Sapphire laser system (Spectra Physics, Spitfire Pro) and an automated data acquisition system (Ultrafast Systems, EOS). The amplifier was seeded with the 120 fs output from the oscillator (Spectra Physics, Tsunami) and was operated at 1.0 kHz for EOS. The output from the amplifier was split 90/10 with the majority used to pump an optical parametric amplifier (Topas) which provided the pump beam. For EOS experiments, a supercontinuum light source (Ultrafast Systems) was used for the probe.

2,9-bis(2,4,6-triisopropylphenyl)-1,10-phenanthroline (bL2): 2,9-Dichloro-1,10-phenanthroline (0.38 g, 1.53 mmol), 2,4,6-triisopropylphenylboronic acid (1.00 g, 4.03 mmol) and $Ba(OH)_2{\cdot}8H_2O$ (3.5 g, 11.09 mmol) were placed in a pressure tube. A dioxane/water mixture (16 mL, 3:1) was added and the reaction was deaerated for 15 minutes. $Pd(PPh_3)_4$ (0.19 g, 0.16 mmol) was added and the reaction was stirred at 115^{o}C for 24 hours. The reaction mixture was allowed to cool to room temperature, was filtered and washed with dichloromethane. Aqueous NaOH solution (5%, 10 mL) was added to the filtrate, the organic layer was separated and the aqueous layer was washed with dichloromethane (2 times). The combined organic fraction was washed with water and brine, dried with Na_2SO_4, filtered and concentrated. Chromatography on silica, eluting with dichloromethane/2 % methanol afforded the product as an off-white solid in 89% yield (0.79 g). ^{1}H NMR ($CDCl_3$): δ 8.25 (2H, d, J = 8.15 Hz); 7.87 (2H, s); 7.59 (2H, d, J = 8.10 Hz); 7.04 (4H, s); 2.92 (2H, septet, J = 7.03 Hz); 2.51 (4H, septet, J = 6.85 Hz); 1.28 (6H, d, J = 6.90 Hz); 1.07 (6H, d, J = 6.90 Hz); 1.06 (6H, d, J = 6.75 Hz). ESI-MS (CH_3OH): calcd $[M+H^+]^+$ 585.42; obsd 585.50; Anal. calcd. for ligand **bL2**, $C_{42}H_{52}N_2{\cdot}1/8CH_2Cl_2$: C, 84.96; H, 8.84; N, 4.70. Found: C, 84.70; H, 8.81; N, 4.59.

Complex 3: $[Cu(CH_3CN)_4]PF_6$ (29.0 mg, 0.078 mmol) was added to a round bottom flask and dissolved in dichloromethane (10 mL) with stirring. The clear colorless solution was deaearated with N_2. A similarly deaerated solution of 2,9-bis(2,4,6-triisopropylphenyl)-1,10-phenanthroline (50 mg, 0.85 mmol) in dichloromethane (5 mL) was added to the reaction mixture. Upon addition of 2,9-bis(2,4,6-triisopropylphenyl)-1,10-phenanthroline, the solution turned bright yellow, and

was allowed to stir at room temperature for one hour. A deaerated solution of 1,10-phenanthroline (14.0 mg, 0.078 mmol) in dichloromethane (5 mL) was then added to the reaction mixture which turned orange/red. The red solution was allowed to stir under N_2 at room temperature for one hour. The solvent was evaporated, the residue was re-dissolved in a minimum volume of dichloromethane and the product precipitated with diethyl ether and pentane. The orange-red solid was isolated by filtration and allowed to dry in air to give complex **3** (59 mg, 0.061 mmol, 78% yield). Single crystals suitable for X-ray structure analysis were obtained via diffusion of diethyl ether into a concentrated dichloromethane product solution. ^{1}H NMR (CD_3Cl): δ 8.67 (d, J = 8.20 Hz, 2H), 8.30-8.25 (m, 4H), 7.89 (d, J = 8.20 Hz, 2H), 7.84 (s, 2H), 7.57 (dd, J = 8.10 Hz, 4.70 Hz, 2H), 6.41 (s, 4H), 2.42 (septet, J = 6.81 Hz, 2H), 2.10 (septet, J = 6.82 Hz, 4H), 0.88 (d, J = 6.80 Hz, 6H), 0.79 (d, J = 6.95 Hz, 6H), 0.37 (d, J = 6.75 Hz, 6H),. ESI-MS (CH_3OH): calcd $[M\text{-}PF_6^-]^+$ 827.41; obsd 827.42. Anal. calcd. for complex **3**, $C_{56}H_{64}CuF_6N_4P\cdot 1/4CH_2Cl_2$: C, 65.50; H, 6.13; N, 5.63. Found: C, 65.52; H, 6.00; N, 5.61.

Complex 4

Method A: The same procedure as described for complex **3** was followed using $[Cu(CH_3CN)_4]PF_6$ (15.9 mg, 0.043 mmol), 2,9-bis(2,4,6-triisopropylphenyl)-1,10-phenanthroline (31 mg, 0.053 mmol) and 2,9-dimethyl-1,10-phenanthroline (8.9 mg, 0.43 mmol). Complex **4** was obtained contaminated with approximately 10% homoleptic $[Cu(dmp)_2]PF_6$. The small impurities of $[Cu(dmp)_2]PF_6$ were removed via recrystallization from a dichloromethane/diethyl ether/pentane mixture to afford pure complex **4** (31 mg, 72% yield). Single crystals suitable for X-ray structure analysis were obtained via diffusion of pentane into a dichloromethane/diethyl ether product solution.

Method B: Under a nitrogen atmosphere copper powder (1.00 g), $AgPF_6$ (22.4 mg; 0.089 mmol) and 2,9-bis(2,4,6-triisopropylphenyl)-1,10-phenanthroline (51.8 mg, 0.089 mmol) were placed in a Schlenk flask. Dry degassed acetone (10 ml) was added and the mixture was stirred for 1.5 hours at room temperature. The reaction mixture was filtered and 2,9-dimethyl-1,10-phenanthroline (18.5 mg, 0.089 mmol) was added to the filtrate. The orange/red solution was stirred for two hours at room temperature and the product was precipitated by adding a diethyl

ether/pentane mixture to the reaction. Filtration and washing with diethyl ether afforded complex **4** without any homoleptic $[Cu(dmp)_2]PF_6$ complex formation (71 mg, 80% yield).

^1H NMR (CD_3Cl): δ 8.69 (d, J = 8.20 Hz, 2H), 8.27 (s, 2H), 8.18 (d, J = 8.20 Hz, 2H), 7.93 (d, J = 8.20 Hz, 2H), 7.78 (s, 2H), 7.39 (d, J = 8.20 Hz, 2H), 6.47 (s, 4H), 2.55 (septet, J = 6.92 Hz, 2H), 2.10 (septet, J = 6.77 Hz, 4H), 1.83 (s, 6H), 0.93 (d, J = 6.90 Hz, 6H), 0.85 (d, J = 6.80 Hz, 6H), 0.23 (d, J = 6.70 Hz, 6H). ESI-MS (CH_3OH): calcd $[M\text{-}PF_6^-]^+$ 855.44; obsd 855.50. Anal. calcd. for complex **4**, $C_{56}H_{64}CuF_6N_4P$: C, 67.15; H, 6.44; N, 5.59. Found: C, 66.81; H, 6.35; N, 5.67.

Results and Discussion

Ligand and CuHETPHEN synthesis. Our previous work on CuHETPHEN model complexes demonstrated that varying the steric bulk of **L** in complexes of the general formula Cu(I)(**bL1**)(**L**) dramatically influenced the excited state lifetime. Therefore, we reasoned that increasing the steric bulk of the 2,9-substitution of **bL** would similarly influence the ground and excited state characteristics of CuHETPHEN complexes and also increase the structural diversity to select from when integrating such complexes into photocatalytic systems. The analogous 2,2'-bipyridine ligand with 6,6'-(di-2,4,6-triisopropyl-phenyl) substitution is known,[40] and our synthesis of the phenanthroline version proceeded similarly via Suzuki coupling of 2,4,6-triisopropyphenyl boronic acid and 2,9-dichloro-1,10-phenanthroline.

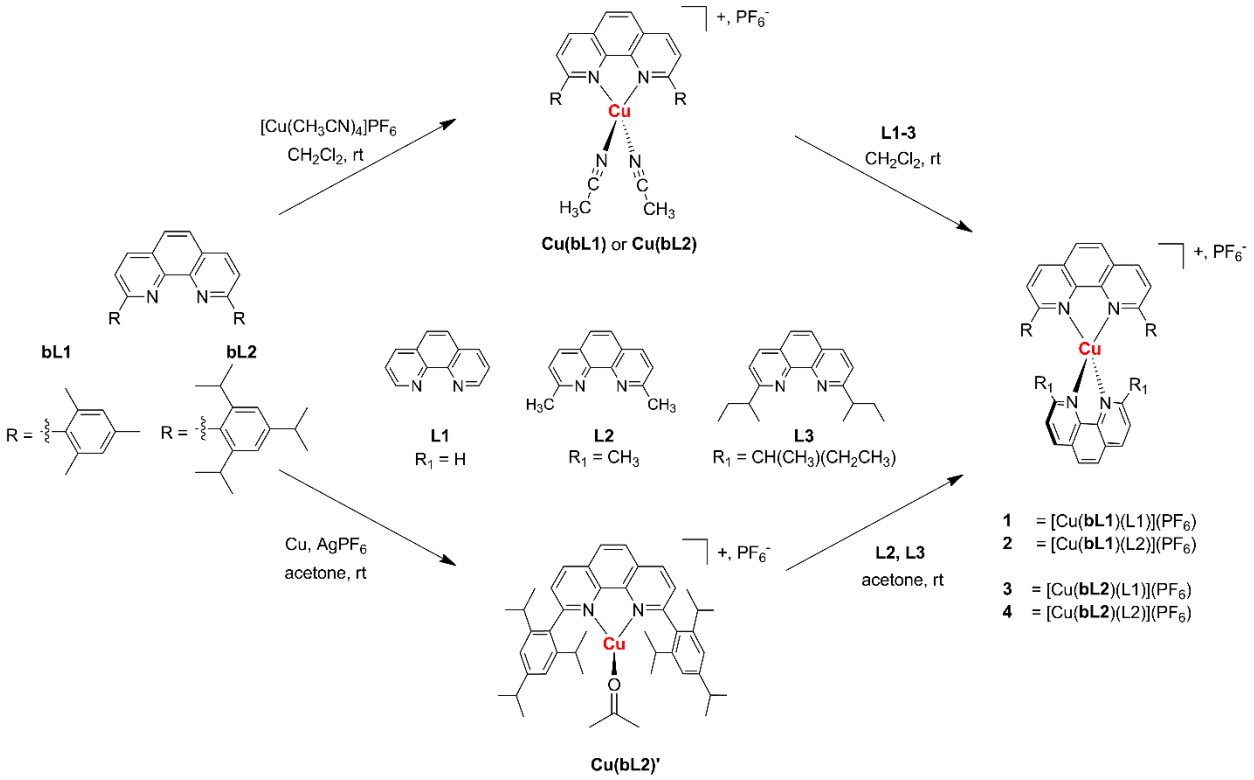

Scheme 1. Synthesis of CuHETPHEN complexes. The top synthesis route follows the typical HETPHEN approach developed by Schmittel and co-workers using the $[Cu(CH_3CN)_4](PF_6)$ reagent. The bottom synthesis route follows the approach developed by Ghandi *et. al.* (ref. 46) via oxidation of Cu(0) in non-coordinating solvents.

Using the general HETPHEN approach developed by Schmittel and co-workers,[41-46] we have obtained pure quantities of heteroleptic Cu(I)(**bL2**)(**L**) complexes incorporating the new ligand **bL2** (Scheme 1). The typical one-pot, two-step synthesis using the common $[Cu(CH_3CN)_4](PF_6)$ precursor proceeded flawlessly for the preparation of complex **3**. However, when 2,9-dimethyl-1,10-phenanthroline (**L2**) was introduced to the reaction mixture containing the $[Cu(\mathbf{bL2})(CH_3CN)_2](PF_6)$ intermediate, we obtained the homoleptic $[Cu(\mathbf{L2})_2](PF_6)$ complex in approximately 10-20% yield. In this case, the homoleptic impurity could be cleanly separated from the desired $[Cu(\mathbf{bL2})(\mathbf{L2})](PF_6)$ by recrystallization from a dichloromethane/diethyl ether/pentane mixture. We also explored an alternative approach to CuHETPHEN synthesis where coordinating solvents are rigorously excluded from the reaction mixture and one equivalent of **bL2** is introduced to a suspension of Cu(0) powder in acetone in the presence of one equivalent of $AgPF_6$.[47] The $[Cu(\mathbf{bL2})(OC(CH_3)_2)](PF_6)$ intermediate was then treated with the

second phenanthroline ligand (**L2** or **L3**) to generate the corresponding HETPHEN complex. In our hands this method resulted in exclusive formation of **4** with no contamination from the homoleptic [Cu(**L2**)$_2$](PF$_6$). Complex **4** was very stable when dissolved in solvents such as dichloromethane, acetone, and methanol, but decomposed quickly in acetonitrile forming homoleptic [Cu(**L2**)$_2$](PF$_6$) as the major product. In attempts to use **L3** as the second phenanthroline ligand and further increase the steric bulk around the Cu(I) center, we observed formation of the corresponding CuHETPHEN complex by mass spectrometry of the reaction mixture. However, the target [Cu(**bL2**)(**L3**)](PF$_6$) complex decomposed quickly in all common solvents and could not be isolated. The instability of the heavily substituted [Cu(**bL2**)(**L3**)]PF$_6$ juxtaposed with the relatively straightforward synthesis and isolation of [Cu(**bL1**)(**L3**)]PF$_6$ that we previously described[36] suggests that we have approached the upper limit of 2,9-substitution possible in CuHETPHEN complexes.

Single crystal structural characterization. The single crystal X-ray structures of the two new CuHETPHEN complexes **3** and **4** are shown in Figure 2. The crystallographic data are summarized in Table 1, and selected interatomic bond lengths and angles are listed in Table 2. Both compounds crystallize in the space group P2$_1$/c. The asymmetric unit of **3** is occupied by one CuHETPHEN molecule and one dichloromethane molecule, and that of **4** is occupied by two independent CuHETPHEN molecules and two diethyl ether molecules. The average Cu-N bond length of **3** and **4** is very similar to that previously reported for **1** and **2** (~2.05 Å). However, more interesting are the individual bond lengths of complexes **3** and **4** containing **bL2**. The Cu-N distances are relatively similar toward **bL2** (2.04-2.07 Å) whereas the Cu-N distances towards **L** skew unusually short (< 2.01 Å) for one bond and unusually long (>2.08 Å) for the other. The longest Cu-N bond length in this series, 2.13 Å, is found in **4**. This long Cu-N bond is likely the main contribution to the instability of **4** in the strongly coordinating solvent acetonitrile, and why the even more sterically congested complex [Cu(**bL2**)(**L3**)](PF$_6$) could not be isolated. Similar stability issues were previously reported for the homoleptic complexes containing the bulky 2,9-di-*tert*-butyl-1,10-phenanthroline ligand, where crystal structures of this compound revealed a Cu-N bond longer than 2.14 Å.[47]

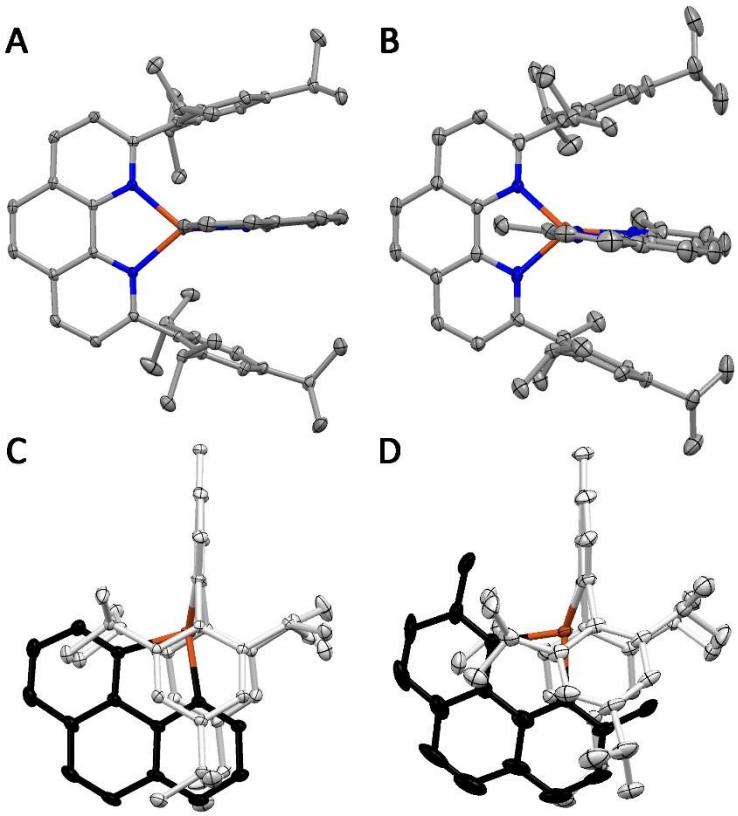

Figure 2. Top: X-ray crystal structures of complexes **3** (A) and **4** (B). Ellipsoids represent 50% probability. Hydrogen atoms, solvent molecules, and counterions are omitted for clarity. Carbon, gray; nitrogen, blue; copper, orange. Bottom: Views along the phenanthroline plane of **bL2** illustrate ligand distortion from tetrahedral geometry around Cu(I) center in **3** (C) and **4** (D). **bL2**, light gray; **L**, black; copper, orange.

Table 1. Crystallographic data for complexes **3** and **4**.

Compound	**3**	**4**
Formula	$C_{55}H_{62}Cl_2CuF_6N_4P$	$C_{60}H_{74}CuF_6N_4OP$
Mw (g mol^{-1})	1058.51	1075.77
Lattice Type	Monoclinic	Monoclinic
Space Group	$P2_1/c$	$P2_1/c$
a (Å)	12.2043(8)	22.851(9)
b(Å)	22.7956(14)	19.517(7)

c(Å)	18.6567(12)	25.628(9)
$\alpha/\beta/\gamma$ (°)	90.00 / 93.2555(9) / 90.00	90.00 / 90.164(5) / 90.00
V (Å^3)	5182.0(6)	11430(7)
Z	4	4
ρ_{calc} (g cm^{-1})	1.357	1.250
T (K)[a]	100	100
λ (Å) [Mo kα]	0.71073	0.71073
μ (mm^{-1})	0.618	0.472
S (GOF)	0.999	1.090
$R(F_o)$, $wR(F_o^2)$	0.037, 0.105	0.082, 0.21

Table 2. Selected bond length, bond angles and geometry index parameter s_4

Compound	**3**	**4**	
		Molecule A	**Molecule B**
	Selected bond length		
Cu1-N1	2.0445(9)	2.126(6)	1.997(5)
Cu1-N2	2.0053(9)	2.005(5)	2.105(6)
Cu1-N3	2.0614(8)	2.073(5)	2.070(5)
Cu1-N4	2.0852(9)	2.051(5)	2.056(6)
	Selected bond angles		
N2-Cu1-N1	138.52(4)	81.7(2)	82.3(2)
N2-Cu1-N4	132.68(4)	133.4(2)	112.9(2)
N1-Cu1-N4	81.81(3)	109.5(2)	137.7(2)
N2-Cu1-N3	82.64(4)	136.6(2)	108.6(2)
N1-Cu1-N3	109.45(3)	114.7(2)	131.5(2)
N4-Cu1-N3	109.84(4)	81.0(2)	82.7(2)
	s_4 values		
	0.630	0.638	0.644

Our group and others have shown that CuHETPHEN complexes based on **bL1** contain a considerable distortion from the tetrahedral geometry expected for Cu(I)diimine complexes. This distortion is directed by π-π interaction between one mesityl group of **bL1** and the B-ring of the secondary phenanthroline ligand (**L**) and results in the so-called "pac-man" motif (Figure 3).[36, 48] In contrast, CuHETPHEN complexes of the general formula [Cu(**bL1**)(bpy)](PF_6), where 2,2'-bipyridine or an analog replaces 1,10-phenanthroline as **L**, do not show this sort of preferential interaction. Rather, these structures reveal two π-π interactions between each mesityl group of **bL1** and the second ligand, where the bipyridine was "clamped" right in the middle of the mesityl groups ("clamped down" motif, Figure 3). The crystal structures of **3** and **4** clearly demonstrate that introducing isopropyl groups instead of methyl groups in the **bL** results in a new type of motif where all inter-ligand π-π interactions are prohibited by the very bulky isopropyl groups of **bL2** ("centered" motif, Figure 3). The distortion of the new CuHETPHEN complexes was quantified using the geometry index parameter s_4:

$$s_4 = \frac{360° - a - b}{141°} \quad (1)$$

where *a* and *b* represent the largest angles in the four coordinate geometry.[49] For a perfect square planar geometry, s_4 = 0, and for a perfect tetrahedral structure s_4 = 1. Analysis of complexes **3** and **4** reveals a greater distortion from tetrahedral geometry (0.63 and 0.64, respectively) in comparison to the **bL1** containing compounds **1** and **2** (0.69 and 0.65, respectively). As with the [Cu(**bL1**)(**L**)](PF_6) complexes that we have previously analyzed, changes of **L** in [Cu(**bL2**)(**L**)](PF_6) had a relatively minor effect on s_4. In the CuHETPHEN complexes, **bL** determines both access to the metal center and inter-ligand interactions, both factors that are important in determining ground and excited state behavior.

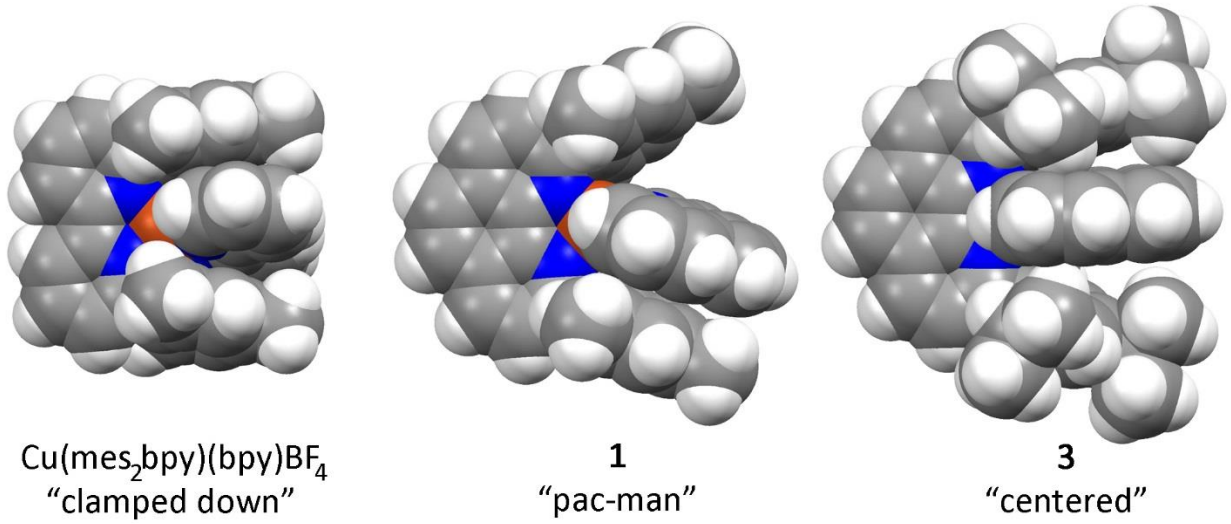

Figure 3. Spacefilling diagrams of complexes Cu(mes$_2$bpy)(bpy)(BF$_4$), **1**, and **3**, illustrating "clamped-down", "pac-man", and "centered" interactions between hetero-ligands coordinated to Cu(I).

Electrochemical properties. The electrochemical behavior of CuHETPHEN complexes containing **bL2** was measured by cyclic voltammetry in dichloromethane (Figure 4). The Cu(II/I) oxidation potentials are well behaved and reversible for each CuHETPHEN complex studied here and are summarized in Table 3. The least sterically congested complex **1** was oxidized at the lowest potential, 0.77 V vs. SCE. Increasing the steric bulk around the Cu(I) center led to a more positive oxidation potential, but the magnitude of increase varied with each phenanthroline ligand (**bL** vs. **L**). Increasing the steric bulk of **bL** results in only a small increase in the Cu(II/I) oxidation potential (30-50 mV), whereas increasing the 2,9-substitution of **L** from hydrogen to methyl increased the Cu(II/I) oxidation potential by ~200 mV. As a result, complex **4** was found to be the most difficult to oxidize at 1.01 V vs. SCE.

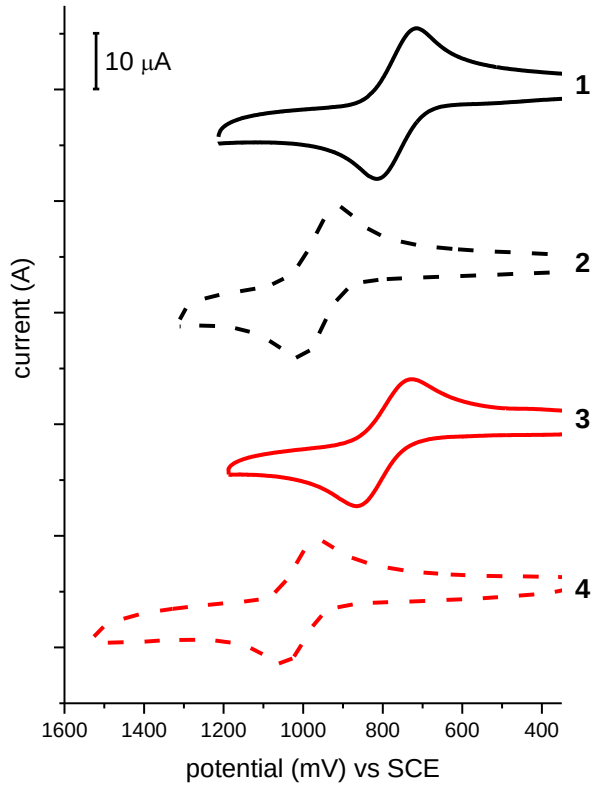

Figure 4. Cyclic voltammograms of 1mM **1**-**4** in 0.1M $TBAPF_6$ / CH_2Cl_2 comparing Cu(I/II) oxidation potentials. Potential is referenced to SCE using ferrocene as an internal standard.

Table 3. Summary of redox and optical characteristics of CuHETPHEN **1**-**4** in CH_2Cl_2 at room temperature. nd = not detected.

complex	$E(Cu^{2+/+})$ (V vs. SCE)	λ_{max} (MLCT, nm)	ε ($M^{-1}cm^{-1}$)	emission max (nm)	E^{00}, eV	$E(Cu^{2+/+*})$ (V vs. SCE)
1	+0.77	467	7326	nd	--	--
2	+0.96	460	5631	686	2.22	-1.26
3	+0.80	461	5253	nd	--	--
4	+1.01	445	4175	671	2.21	-1.20

Absorption and emission spectroscopy. The UV-Vis absorption spectra of complexes **1**-**4** were measured in dichloromethane and are shown in Figure 5 and summarized in Table 3. All

complexes exhibit a broad absorption band around 460 nm, which is associated with MLCT from Cu(I) to the phenanthroline ligands. We observe a blue shift of the MLCT band in response to the increasing steric hindrance around the Cu(I) center by modifying both **bL** and **L**. For example, changing from **bL1** to **bL2** and keeping **L** constant resulted in a 6 nm blue shift between the **L1** containing complexes **1** and **3** and a 15 nm shift between the **L2** containing complexes **2** and **4**. The difference in MLCT peak maximum between the complexes carrying **bL1** is smaller than the complexes containing **bL2** (7 nm vs. 16 nm). We found a strong correlation between the sterics of the CuHETPHEN complexes and their absorption intensities. The least sterically congested complex **1** absorbs most strongly in the visible, and complex **4**, carrying the bulkiest substituents, most weakly. The decrease in extinction coefficient is correlated with the increasing distortion from tetrahedral geometry (from D_{2d} to D_2) as observed in the crystal structures.

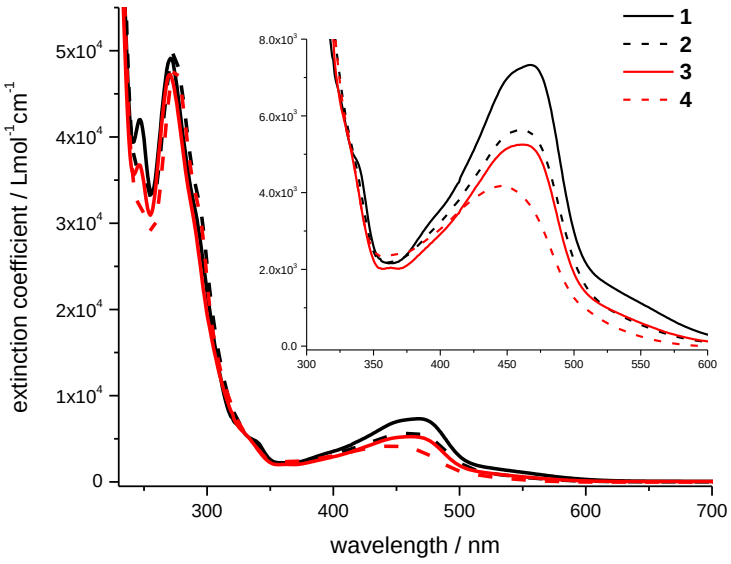

Figure 5. UV-Vis absorption spectra of complexes **1**-**4** in dichloromethane.

To understand the impact of **bL2** on the excited state properties, the emission spectra of **1**-**4** were measured at room temperature in dichloromethane (Figure S1). Complexes **1** and **3** carrying the unsubstituted phenanthroline ligand **L1** showed no measureable emission at room temperature following excitation of the MLCT band, which has been noted previously for relatively unsubstituted CuHETPHEN complexes.[29] However, when the steric bulk near the Cu(I)

center is increased by coordination of **L2**, as in complexes **2** and **4**, we observe weak emission spectra following MLCT excitation. The E^{00} energy is determined by extending a tangent from the blue side of the emission spectra to y = 0 and the excited state reduction potential can then be calculated using Equation 2:

$$E(Cu^{2+/+*}) = E(Cu^{2+/+}) - E^{00} \quad (2)$$

The excited state reduction potentials of **2** and **4** are similar, -1.26 and -1.20V vs. SCE, and in good agreement with values previously reported for homoleptic and heteroleptic Cu(I)diimine complexes.[29, 34, 36]

Transient absorption spectroscopy. To understand the excited state kinetics of CuHETPHEN complexes **1**-**4**, we performed room temperature ultrafast (femtosecond) and nanosecond transient absorption spectroscopy in both methanol and dichloromethane as representative coordinating and non-coordinating solvents. Overall, the TA spectra of **1**-**4** in both solvents resemble that typically found of Cu(I)diimine complexes,[34, 36, 38, 50] and the spectra of **3** and **4** in methanol are shown in Figure 6 to illustrate the relevant features. Immediately following excitation of the MLCT band at 415 nm, we observe a negative feature at 460 nm associated with the ground state bleach and a broad positive feature centered at 550 nm that is correlated with the formation of a Cu(II)-based ^{1}MLCT charge separated state. This broad positive feature transitions into a well-resolved double-headed feature in the first few picoseconds with peaks centered at 514 and 554nm, which is attributed to the radical anion spectra of the phenanthroline ligands. The double-headed feature then decays to the ground state on the nanosecond time scale. The kinetics of the ground state bleach and excited state absorption features were modeled using a global fit to a three-component exponential decay function, with the three components corresponding to: Jahn-Teller distortion (flattening) in the ^{1}MLCT Cu(II) excited state (τ_1); ISC from ^{1}MLCT to ^{3}MLCT (τ_2); and ^{3}MLCT decay to the ground state (τ_3). A summary of the kinetic parameters for all CuHETPHEN complexes in both solvents is given in Table 4 and fitting details are in the Supporting Information.

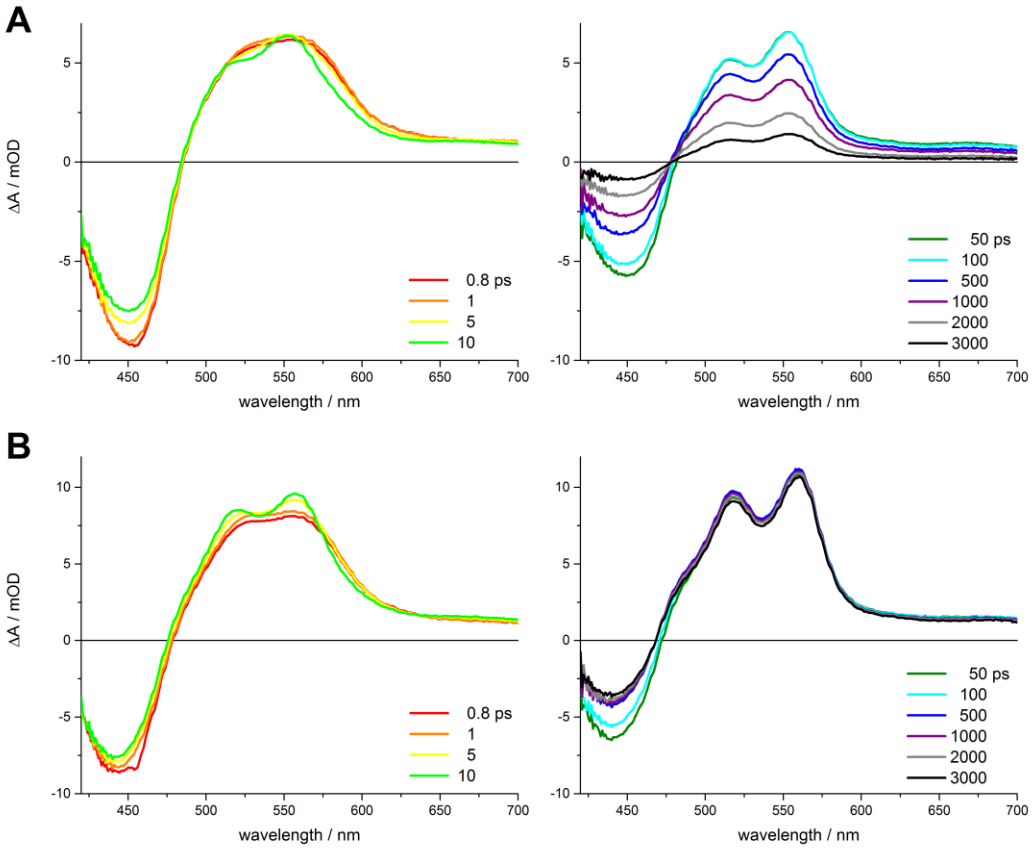

Figure 6. Comparison of ultrafast transient absorption spectra of CuHETPHEN (A) **3** and (B) **4** following 415nm excitation in methanol. Left panels depict early transient spectra up to 10 ps; right panels show transient spectra from 50 - 3000 ps.

Table 4. Summary of excited state kinetics for CuHETPHEN **1**-**4** in non-coordinating (CH_2Cl_2) and coordinating (CH_3OH) solvents.

	CH_2Cl_2			CH_3OH		
Complex	**τ_1 (ps)**	**τ_2 (ps)**	**τ_3 (ns)**	**τ_1 (ps)**	**τ_2 (ps)**	**τ_3 (ns)**
1	0.32 ± 0.01	18.3 ± 0.2	3.43 ± 0.06	0.18 ± 0.01	18.0 ± 0.1	1.18 ± 0.02
2	0.31 ± 0.01	18.0 ± 0.1	46.8 ± 0.3	0.22 ± 0.01	19.0 ± 0.2	24.7 ± 0.2
3	0.29 ± 0.01	20.5 ± 0.8	4.05 ± 0.07	0.21 ± 0.01	20.8 ± 0.2	1.85 ± 0.05
4	0.35 ± 0.01	25.0 ± 0.7	68.2 ± 0.4	0.20 ± 0.01	24.9 ± 0.5	35.6 ± 0.3

The excited state kinetics of CuHETPHEN complexes are readily modulated by both solvent and ligand substitution, as has been demonstrated for homoleptic Cu(I)diimine complexes. The excited state kinetics of CuHETPHEN complexes **1**-**4** in the coordinating solvent methanol show an interesting response to ligand structural modifications. Within the temporal resolution of our ultrafast TA set-up, we do not observe a difference in the earliest decay component, τ_1, which suggests that the Jahn-Teller flattening distortion following ^{1}MLCT generation is not influenced dramatically by either the 2,9-substitution of **L** or increasing the steric bulk of **bL** from trimethyl to triisopropyl.[51] The second decay component, τ_2, which is attributed to ISC to generate the ^{3}MLCT state, does show a small positive correlation with steric bulk. The least substituted CuHETPHEN **1** has the shortest decay component (τ_2 = 18.0 ps) and the most heavily substituted CuHETPHEN **4** has the longest decay component (τ_2 = 24.9 ps). Unlike the other kinetic components, decay from the ^{3}MLCT state does show a significant dependence on the ligand sterics. As documented in recent review articles,[30-31] τ_3 increases substantially when increasing the substitution at the 2,9-position of L; we observe an approximately 20-fold increase in ^{3}MLCT lifetime in going from hydrogen to methyl substitution (comparing **1** vs. **2** and **3** vs. **4**). The effect of **bL** sterics on ^{3}MLCT lifetime is less dramatic (comparing **1** vs. **3** and **2** vs. **4**), but there is still an increase in lifetime of about 50% in going from **bL1** to **bL2**, demonstrating that even the remote ligand structural features influence excited state kinetics.

X-ray transient absorption studies have proven that Cu(I)diimine complexes in the charge-separated state have some interaction with solvent molecules capable of metal ligation.[52-55] Therefore, in this work we measured the excited state kinetics for **1**-**4** in a non-coordinating solvent (dichloromethane) and a coordinating solvent (methanol) to understand how the ligand modifications influence solvent access and excited state kinetics. The Jahn-Teller flattening distortion in the Cu(II) ^{1}MLCT state is slightly slower in dichloromethane than in methanol (τ_1 ~0.3 ps in CH_2Cl_2, ~0.2 ps in CH_3OH), which could be a result of better charge stabilization in a polar solvent such as methanol as opposed to the relatively non-polar dichloromethane. Interestingly, the time constant attributed to ISC is nearly identical for each complex in both solvents,

suggesting that the singlet-triplet gap is solvent independent. As noted previously for Cu(I)diimine complexes, the ^{3}MLCT decay is highly solvent dependent.[56] The ^{3}MLCT decay lifetime of **1**-**4** in methanol followed a similar trend as in dichloromethane, but the τ_3 values were two to three times shorter. This behavior can be explained by solvent accessibility and interaction with solvent molecules that accelerates ^{3}MLCT-state decay.

Conclusions

Here we have described the synthesis of a new phenanthroline ligand (**bL2**) with sterically-demanding 2,4,6-tri-isopropyl-phenyl groups appended to the 2,9-phenanthroline positions. We anticipate that this ligand will be useful in the development of transition metal complexes whose properties are dependent on controlling small molecule access to the metal site. To demonstrate this effect, we synthesized two new heteroleptic Cu(I)diimine complexes using **bL2** to prevent homoleptic coordination in place of the more commonly used **bL1**, which features 2,9-mesityl substitution. Analysis of the single crystal X-ray structures clearly shows that the increase in steric bulk of **bL2** positions the secondary phenanthroline ligand in a more "centered" configuration and prevents the inter-ligand π-π interaction which is observed in CuHETPHEN complexes containing **bL1**. The substitution of **bL2** for **bL1** in CuHETPHEN complexes results in moderate changes to the ground state redox and optical properties. With the increased steric bulk of **bL2**, the Cu(I/II) oxidation potential increases slightly (30-50 mV), and the MLCT absorption band shifts to slightly higher energy (5-6 nm) but decreases in intensity by approximately 30%. The excited state reduction potential of CuHETPHEN **4** is -1.20 V vs. SCE, aligned with that reported for related Cu(I)diimine complexes, and is notably a much stronger photoreductant than the common photosensitizer $Ru(bpy)_3^{2+}$.[57] Transient optical spectroscopy was used to determine the excited state kinetics of the CuHETPHEN complexes in methanol and dichloromethane as representative coordinating and non-coordinating solvents. In general, the blocking ligand does not have a dramatic effect on the early kinetics, which are attributed to the flattening distortion in the ^{1}MLCT state (τ_1) and ISC (τ_2). However, the lifetime of the ^{3}MLCT excited state increases by ~50% from CuHETPHEN complexes containing **bL1** to those with **bL2**, indicating that the change from methyl to isopropyl substitution, even far removed from the copper center, influences how solvent molecules interact with the metal site and thereby affect

photophysical properties. In summary, this work adds to the growing library of CuHETPHEN complexes and the fundamental understanding of their ground and excited state properties. Current research is focused on the integration of CuHETPHEN complexes into molecular systems based on earth-abundant elements for light-harvesting and solar energy conversion.

Acknowledgments

This work is supported by the Division of Chemical Sciences, Geosciences, and Biosciences, Office of Basic Energy Sciences of the U.S. Department of Energy through Grant DE-AC02-06CH11357. DH acknowledges support from the ANL Joseph J. Katz Fellowship. We acknowledge Dr. Richard E. Wilson for assistance in collecting the X-ray diffraction data. Use of the Center for Nanoscale Materials, an Office of Science user facility, was supported by the U.S. Department of Energy, Office of Science, Office of Basic Energy Sciences, under Contract No. DE-AC02-06CH11357. We thank Dr. David J. Gosztola for his expert assistance at the transient absorption facility at CNM.

References

1. Cotton, F. A.; Wilkinson, G.; Bochmann, M.; Murillo, C., *Advanced Inorganic Chemistry, 6th Edition*. Wiley: 1998; p 1248 pp.
2. Fromm, K. M. In *Coordination compounds*, John Wiley & Sons, Inc.: 2004; pp 573-606.
3. Balzani, V.; Campagna, S., *Photochemistry and Photophysics of Coordination Compounds I*. 2007; Vol. 280.
4. Balzani, V.; Campagna, S., *Photochemistry and Photophysics of Coordination Compounds II*. 2007; Vol. 281.
5. Werner, A., The Asymmetric Cobalt Atom. V. *Ber. Dtsch. Chem. Ges.* **1912,** *45*, 121-30.
6. Werner, A., Stereoisomeric Cobalt Compounds. *Annalen der Chemie, Justus Liebigs* **1912,** *386*, 1-272.
7. Tolman, C. A., Steric effects of phosphorus ligands in organometallic chemistry and homogeneous catalysis. *Chem. Rev.* **1977,** *77* (3), 313-348.
8. Keim, W., Coordination geometry and bio-inspired ligands: useful concepts in homogeneous catalysis? A conceptual view. *J. Mol. Catal. A: Chem.* **2004,** *224* (1-2), 11-16.
9. Dempsey, J. L.; Esswein, A. J.; Manke, D. R.; Rosenthal, J.; Soper, J. D.; Nocera, D. G., Molecular Chemistry of Consequence to Renewable Energy. *Inorg. Chem.* **2005,** *44* (20), 6879-6892.
10. DuBois, M. R.; DuBois, D. L., The roles of the first and second coordination spheres in the design of molecular catalysts for H2 production and oxidation. *Chem. Soc. Rev.* **2009,** *38* (1), 62-72.
11. Shook, R. L.; Borovik, A. S., Role of the Secondary Coordination Sphere in Metal-Mediated Dioxygen Activation. *Inorg. Chem.* **2010,** *49* (8), 3646-3660.
12. Mercer, D. J.; Loeb, S. J., Metal-based anion receptors: An application of second-sphere coordination. *Chem. Soc. Rev.* **2010,** *39* (10), 3612-3620.
13. Shul'pin, G. B., C-H functionalization: thoroughly tuning ligands at a metal ion, a chemist can greatly enhance catalyst's activity and selectivity. *Dalton Trans.* **2013,** *42* (36), 12794-12818.

14. Liu, Z.; Schneebeli, S. T.; Stoddart, J. F., Second-sphere coordination revisited. *Chimia* **2014,** *68* (5), 315-320.
15. Mulfort, K. L.; Utschig, L. M., Modular Homogeneous Chromophore–Catalyst Assemblies. *Acc. Chem. Res.* **2016,** *49* (5), 835-843.
16. Dinolfo, P. H.; Hupp, J. T., Supramolecular Coordination Chemistry and Functional Microporous Molecular Materials. *Chem. Mater.* **2001,** *13* (10), 3113-3125.
17. Holliday, B. J.; Mirkin, C. A., Strategies for the construction of supramolecular compounds through coordination chemistry. *Angew. Chem., Int. Ed.* **2001,** *40* (11), 2022-2043.
18. Telfer, S. G.; Kuroda, R., 1,1'-Binaphthyl-2,2'-diol and 2,2'-diamino-1,1'-binaphthyl: versatile frameworks for chiral ligands in coordination and metallosupramolecular chemistry. *Coord. Chem. Rev.* **2003,** *242* (1-2), 33-46.
19. Cronin, L., Macrocyclic and supramolecular coordination chemistry. *Annu. Rep. Prog. Chem., Sect. A: Inorg. Chem.* **2003,** *99*, 289-347.
20. Kitagawa, S.; Kitaura, R.; Noro, S.-i., Functional porous coordination polymers. *Angew. Chem., Int. Ed.* **2004,** *43* (18), 2334-2375.
21. Ward, M. D., Polynuclear coordination cages. *Chem. Commun. (Cambridge, U. K.)* **2009,** (30), 4487-4499.
22. Farha, O. K.; Hupp, J. T., Rational Design, Synthesis, Purification, and Activation of Metal-Organic Framework Materials. *Acc. Chem. Res.* **2010,** *43* (8), 1166-1175.
23. Kruger, P. E., Coordination polymers and metal-organic frameworks derived from 4,4'-dicarboxy-2,2'-bipyridine and 4,4',6,6'-tetracarboxy-2,2'-bipyridine ligands: a personal perspective. *Chimia* **2013,** *67* (6), 403-410.
24. Harris, K.; Fujita, D.; Fujita, M., Giant hollow MnL2n spherical complexes: structure, functionalisation and applications. *Chem. Commun. (Cambridge, U. K.)* **2013,** *49* (60), 6703-6712.
25. Housecroft, C. E., Divergent 4,2':6',4''- and 3,2':6',3''-terpyridines as linkers in 2- and 3-dimensional architectures. *CrystEngComm* **2015,** *17* (39), 7461-7468.
26. Cook, T. R.; Stang, P. J., Recent Developments in the Preparation and Chemistry of Metallacycles and Metallacages via Coordination. *Chem. Rev. (Washington, DC, U. S.)* **2015,** *115* (15), 7001-7045.
27. Lazorski, M. S.; Castellano, F. N., Advances in the light conversion properties of Cu(I)-based photosensitizers. *Polyhedron* **2014,** *82*, 57-70.
28. Sandroni, M.; Pellegrin, Y.; Odobel, F., Heteroleptic bis-diimine copper(I) complexes for applications in solar energy conversion. *Comptes Rendus Chimie* **2016,** *19* (1–2), 79-93.
29. Scaltrito, D. V.; Thompson, D. W.; O'Callaghan, J. A.; Meyer, G. J., MLCT excited states of cuprous bis-phenanthroline coordination compounds. *Coord. Chem. Rev.* **2000,** *208* (1), 243-266.
30. Lavie-Cambot, A.; Cantuel, M.; Leydet, Y.; Jonusauskas, G.; Bassani, D. M.; McClenaghan, N. D., Improving the photophysical properties of copper(I) bis(phenanthroline) complexes. *Coord. Chem. Rev.* **2008,** *252* (23–24), 2572-2584.
31. Mara, M. W.; Fransted, K. A.; Chen, L. X., Interplays of excited state structures and dynamics in copper(I) diimine complexes: Implications and perspectives. *Coord. Chem. Rev.* **2015,** *282*, 2-18.
32. Iwamura, M.; Takeuchi, S.; Tahara, T., Ultrafast Excited-State Dynamics of Copper(I) Complexes. *Acc. Chem. Res.* **2015,** *48* (3), 782-791.
33. McCusker, C. E.; Castellano, F. N., Design of a Long-Lifetime, Earth-Abundant, Aqueous Compatible Cu(I) Photosensitizer Using Cooperative Steric Effects. *Inorg. Chem.* **2013,** *52* (14), 8114-8120.
34. Garakyaraghi, S.; Crapps, P. D.; McCusker, C. E.; Castellano, F. N., Cuprous Phenanthroline MLCT Chromophore Featuring Synthetically Tailored Photophysics. *Inorg. Chem.* **2016,** *55* (20), 10628-10636.
35. Cunningham, C. T.; Cunningham, K. L. H.; Michalec, J. F.; McMillin, D. R., Cooperative Substituent Effects on the Excited States of Copper Phenanthrolines. *Inorg. Chem.* **1999,** *38* (20), 4388-4392.

36. Kohler, L.; Hayes, D.; Hong, J.; Carter, T. J.; Shelby, M. L.; Fransted, K. A.; Chen, L. X.; Mulfort, K. L., Synthesis, structure, ultrafast kinetics, and light-induced dynamics of CuHETPHEN chromophores. *Dalton Trans.* **2016,** *45*, 9871-9883.
37. Sandroni, M.; Kayanuma, M.; Planchat, A.; Szuwarski, N.; Blart, E.; Pellegrin, Y.; Daniel, C.; Boujtita, M.; Odobel, F., First application of the HETPHEN concept to new heteroleptic bis(diimine) copper(I) complexes as sensitizers in dye sensitized solar cells. *Dalton Trans.* **2013,** *42* (30), 10818-10827.
38. Sandroni, M.; Maufroy, A.; Rebarz, M.; Pellegrin, Y.; Blart, E.; Ruckebusch, C.; Poizat, O.; Sliwa, M.; Odobel, F., Design of Efficient Photoinduced Charge Separation in Donor-Copper(I)-Acceptor Triad. *J. Phys. Chem. C* **2014,** *118* (49), 28388-28400.
39. Connelly, N. G.; Geiger, W. E., Chemical redox agents for organometallic chemistry. *Chem. Rev.* **1996,** *96* (2), 877-910.
40. Benson, E. E.; Rheingold, A. L.; Kubiak, C. P., Synthesis and Characterization of 6,6'-(2,4,6-Triisopropylphenyl)-2,2'-bipyridine (tripbipy) and Its Complexes of the Late First Row Transition Metals. *Inorg. Chem.* **2010,** *49* (4), 1458-1464.
41. Schmittel, M.; Ganz, A., Stable mixed phenanthroline copper(i) complexes. Key building blocks for supramolecular coordination chemistry. *Chem. Commun.* **1997,** (11), 999-1000.
42. Schmittel, M.; Luning, U.; Meder, M.; Ganz, A.; Michel, C.; Herderich, M., Synthesis of sterically encumbered 2,9-diaryl substituted phenanthrolines. Key building blocks for the preparation of mixed (bis-heteroleptic) phenanthroline copper(I) complexes (I). *Heterocycl. Commun.* **1997,** *3* (6), 493-498.
43. Schmittel, M.; Kalsani, V.; Fenske, D.; Wiegrefe, A., Self-assembly of heteroleptic [2 x 2] and [2 x 3] nanogrids. *Chem. Commun.* **2004,** (5), 490-491.
44. Schmittel, M.; Kishore, R. S. K.; Bats, J. W., Synthesis of supramolecular fullerene-porphyrin-Cu(phen)(2)-ferrocene architectures. A heteroleptic approach towards tetrads. *Org Biomol Chem* **2007,** *5* (1), 78-86.
45. De, S.; Mahata, K.; Schmittel, M., Metal-coordination-driven dynamic heteroleptic architectures. *Chem. Soc. Rev.* **2010,** *39* (5), 1555-1575.
46. Neogi, S.; Schnakenburg, G.; Lorenz, Y.; Engeser, M.; Schmittel, M., Implications of Stoichiometry-Controlled Structural Changeover Between Heteroleptic Trigonal [Cu(phenAr2)(py)]+ and Tetragonal [Cu(phenAr2)(py)2]+ Motifs for Solution and Solid-State Supramolecular Self-Assembly. *Inorg. Chem.* **2012,** *51* (20), 10832-10841.
47. Gandhi, B. A.; Green, O.; Burstyn, J. N., Facile Oxidation-Based Synthesis of Sterically Encumbered Four-Coordinate Bis(2,9-di-tert-butyl-1,10-phenanthroline)copper(I) and Related Three-Coordinate Copper(I) Complexes. *Inorg. Chem.* **2007,** *46* (10), 3816-3825.
48. Fraser, M. G.; van der Salm, H.; Cameron, S. A.; Blackman, A. G.; Gordon, K. C., Heteroleptic Cu(I) Bis-diimine Complexes of 6,6'-Dimesityl-2,2'-bipyridine: A Structural, Theoretical and Spectroscopic Study. *Inorg. Chem.* **2013,** *52* (6), 2980-2992.
49. Yang, L.; Powell, D. R.; Houser, R. P., Structural variation in copper(I) complexes with pyridylmethylamide ligands: structural analysis with a new four-coordinate geometry index, tau(4). *Dalton Trans.* **2007,** (9), 955-964.
50. Garakyaraghi, S.; Danilov, E. O.; McCusker, C. E.; Castellano, F. N., Transient Absorption Dynamics of Sterically Congested Cu(I) MLCT Excited States. *J. Phys. Chem. A* **2015,** *119* (13), 3181-3193.
51. However, given that the values of t1 reported in Table 4 are within the instrument response function of our ultrafast TA set-up, we cannot unambiguously rule out the possibility that the true values are shorter or have some meaningful variation on the sub-200 fs timescale.
52. Chen, L. X.; Shaw, G. B.; Novozhilova, I.; Liu, T.; Jennings, G.; Attenkofer, K.; Meyer, G. J.; Coppens, P., MLCT State Structure and Dynamics of a Copper(I) Diimine Complex Characterized by

Pump−Probe X-ray and Laser Spectroscopies and DFT Calculations. *J. Am. Chem. Soc.* **2003,** *125* (23), 7022-7034.
53. Shaw, G. B.; Grant, C. D.; Shirota, H.; Castner, E. W.; Meyer, G. J.; Chen, L. X., Ultrafast Structural Rearrangements in the MLCT Excited State for Copper(I) bis-Phenanthrolines in Solution. *J. Am. Chem. Soc.* **2007,** *129* (7), 2147-2160.
54. Chen, L. X.; Zhang, X., Photochemical Processes Revealed by X-ray Transient Absorption Spectroscopy. *J. Phys. Chem. Lett.* **2013,** *4* (22), 4000-4013.
55. Smolentsev, G.; Sundström, V., Time-resolved X-ray absorption spectroscopy for the study of molecular systems relevant for artificial photosynthesis. *Coord. Chem. Rev.* **2015,** *304–305*, 117-132.
56. Lockard, J. V.; Kabehie, S.; Zink, J. I.; Smolentsev, G.; Soldatov, A.; Chen, L. X., Influence of Ligand Substitution on Excited State Structural Dynamics in Cu(I) Bisphenanthroline Complexes†. *The Journal of Physical Chemistry B* **2010,** *114* (45), 14521-14527.
57. Kalyanasundaram, K., Photophysics, photochemistry and solar energy conversion with tris(bipyridyl)ruthenium(II) and its analogues. *Coord. Chem. Rev.* **1982,** *46*, 159-244.